Mixotrophic basis of Atlantic oligotrophic ecosystems

Manuela Hartmann[a], Carolina Grob[b], Glen A. Tarran[c], Adrian P. Martin[a], Peter H. Burkill[d,e], David J. Scanlan[b], and Mikhail V. Zubkov[a,1]

[a]Ocean Biogeochemistry and Ecosystems Research Group, National Oceanography Centre, Southampton SO14 3ZH, United Kingdom; [b]School of Life Sciences, University of Warwick, Coventry CV4 7AL, United Kingdom; [c]Plymouth Marine Laboratory, Plymouth PL1 3DH, United Kingdom; [d]Sir Alister Hardy Foundation for Ocean Science, Plymouth PL1 2PB, United Kingdom; and [e]Marine Institute, University of Plymouth, Plymouth PL4 8AA, United Kingdom

Edited by David M. Karl, University of Hawaii, Honolulu, HI, and approved March 6, 2012 (received for review November 4, 2011)

Oligotrophic subtropical gyres are the largest oceanic ecosystems, covering >40% of the Earth's surface. Unicellular cyanobacteria and the smallest algae (plastidic protists) dominate CO_2 fixation in these ecosystems, competing for dissolved inorganic nutrients. Here we present direct evidence from the surface mixed layer of the subtropical gyres and adjacent equatorial and temperate regions of the Atlantic Ocean, collected on three Atlantic Meridional Transect cruises on consecutive years, that bacterioplankton are fed on by plastidic and aplastidic protists at comparable rates. Rates of bacterivory were similar in the light and dark. Furthermore, because of their higher abundance, it is the plastidic protists, rather than the aplastidic forms, that control bacterivory in these waters. These findings change our basic understanding of food web function in the open ocean, because plastidic protists should now be considered as the main bacterivores as well as the main CO_2 fixers in the oligotrophic gyres.

phytoplankton predation | phototrophic eukaryotes | primary producers | microbial grazers | pulse–chase labeling

Oligotrophic ecosystems of subtropical oceanic gyres are the most extensive ecosystems on Earth. These ecosystems cover ~40% of the planet's surface, with their area currently expanding (1). *Prochlorococcus* cyanobacteria and the SAR11 group of α-proteobacteria are the most numerous microbes in these ecosystems (2, 3), whereas the smallest plastidic protists, comprising various taxonomic groups including uncultured members of the Prymnesiophyceae and Chrysophyceae (4–8), are the most numerous among the eukaryotes, dominating over their aplastidic counterparts (9). The large area of these oligotrophic gyres means that they play a key role in global biogeochemical cycles. However, current knowledge about the functioning of these microbe-controlled systems is relatively limited, owing to the difficulty of studying microbes in a photic layer typified by nanomolar concentrations of inorganic macronutrients.

According to our current understanding of oligotrophic ecosystem functioning, the roles of different microbial populations are tightly defined. In the established paradigm (10) for these systems, phytoplankton such as cyanobacteria and plastidic protists harvest light, fix CO_2, and take up inorganic nutrients. They are the primary producers of organic matter that fuels the entire system, allowing heterotrophic bacterioplankton, dominated by the SAR11 group, to thrive. Populations of both cyanobacteria and heterotrophic bacterioplankton are controlled by viruses and aplastidic protist predators. Organic matter and inorganic nutrients, released by these control processes, in addition to cell death and bacterioplankton remineralization of dissolved organic matter, sustain heterotrophic bacterioplankton and phytoplankton. However, some more recent observations are at variance with this paradigm.

It is generally accepted that prokaryotes are more efficient than protists in acquiring nutrients at low concentration because of their higher cell surface-to-volume ratio (11). Indeed, in the North Atlantic subtropical gyre, bacterioplankton dominate phosphate uptake and outcompete protists for this nutrient (12, 13). However, despite their low phosphate uptake, plastidic protists are major contributors to CO_2 fixation (5, 14). Consequently, the C:P ratio, calculated using CO_2 and phosphate uptake rates by plastidic protists, is unrealistically high, suggesting that osmotrophic uptake of phosphate cannot satisfy protist requirements for growth (12). Therefore, to sustain themselves in oligotrophic ecosystems, plastidic protists must somehow be able to compensate for a lack of inorganic nutrients. We hypothesize that they do this by mixotrophy: They gain energy from sunlight and simultaneously prey on bacterioplankton to acquire inorganic, and perhaps some essential organic, nutrients, such as amino acids and vitamins.

Mixotrophy in natural populations of large (>3 μm) plastidic protists has been previously documented microscopically in coastal oligotrophic and upwelling regions as well as in the open equatorial Pacific Ocean and the Mediterranean Sea (15–17). There is also qualitative molecular evidence from the subtropical North Pacific of the presence of mixotrophs among picocyanobacterial predators (18). Furthermore, the quantitative dominance of bacterivory by small plastidic protists (<3 μm) over aplastidic protists has been reported for the temperate North Atlantic Ocean in summer (19). The latter paper also outlines preliminary evidence of bacterivory by plastidic protists in the mesotrophic subtropical northeast Atlantic Ocean. However, the ecological extent of mixotrophy in the vast ecosystems of the oligotrophic open ocean remains unknown.

Here we show that plastidic protists prey on bacterioplankton in the surface mixed layer of both oligotrophic subtropical gyres and adjoining low-latitude pelagic regions of the Atlantic Ocean (40°N to 40°S). Owing to their high abundance, plastidic protists prevail over aplastidic protists in bacterivory. This evidence suggests that mixotrophy is crucial to sustain the functioning of oligotrophic marine ecosystems.

Results

Protist bacterivory was assessed on three Atlantic Meridional Transect (AMT) research cruises in October–November 2008, 2009, and 2010 encompassing subtropical oligotrophic gyres of the Northern and Southern hemispheres and the equatorial convergence area (Fig. 1). Temperate waters adjoining the Southern gyre were also examined. The results of an earlier study conducted in 2007 in North Atlantic temperate waters (19) are included for comparison.

Protist feeding on bacterioplankton (Bpl) was determined using a dual-labeling pulse–chase method (20) and flow cytometric sorting of labeled prey and predator cells (19, 21). Three populations of the smallest planktonic protists were examined (Fig. S1): plastidic protists (i.e., chloroplast-containing) smaller, ~2 μm (Plast-S) and larger, ~3 μm (Plast-L) as well as aplastidic (without chloroplast) protists, ~3 μm (Aplast) (Table S1). The two size

Author contributions: A.P.M., P.H.B., D.J.S., and M.V.Z. designed research; M.H., C.G., G.A.T., and M.V.Z. performed research; M.H., G.A.T., and M.V.Z. analyzed data; and M.H., A.P.M., P.H.B., D.J.S., and M.V.Z. wrote the paper.

The authors declare no conflict of interest.

This article is a PNAS Direct Submission.

[1]To whom correspondence should be addressed. E-mail: mvz@noc.ac.uk.

This article contains supporting information online at www.pnas.org/lookup/suppl/doi:10.1073/pnas.1118179109/-/DCSupplemental.

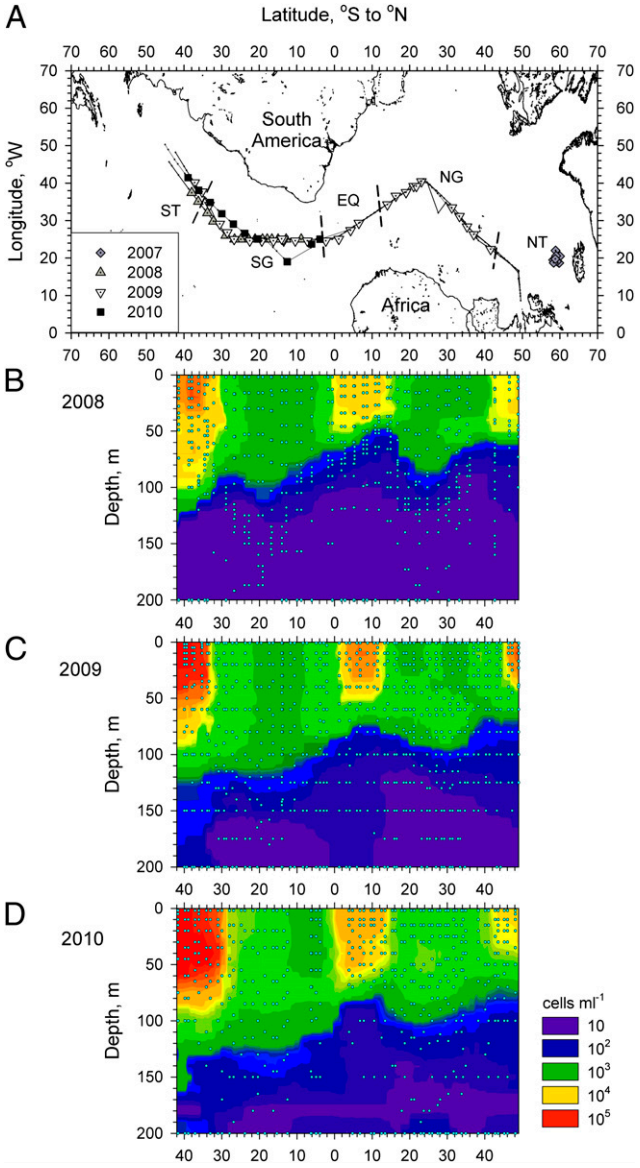

Fig. 1. A schematic map of the Atlantic Ocean showing the area sampled in the 2008, 2009, and 2010 cruises (*A*) with corresponding contour plots of the vertical distribution of *Synechococcus* cyanobacteria in 2008 (*B*), 2009 (*C*), and 2010 (*D*). These distributions were used to identify the boundaries of the five oceanic regions: Northern temperate waters, Northern subtropical gyre, equatorial waters, Southern subtropical gyre, and Southern temperate waters. Short dashed lines (*A*) indicate these boundaries. Solid lines with dots (*A*) indicate the ship tracks and sampled stations, respectively. Circles (*B–D*) indicate sampled depths. The stations sampled in 2007 in North Atlantic temperate waters are also indicated.

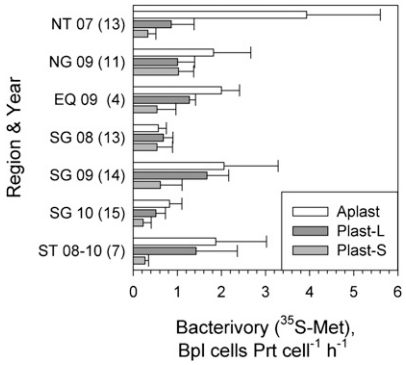

Fig. 2. A comparison of mean rates of cell bacterivory by flow-sorted aplastidic, large plastidic, and small plastidic protists in the five regions (see Fig. 1 for details). The numbers next to the region abbreviations indicate the year of sampling, and the numbers in parentheses indicate the number of separate experiments performed in each region. The rates were calculated using [^{35}S]methionine pulse–chase tracing. Error bars show single SDs to indicate the variance of rates within regions. The results of an earlier study conducted in 2007 in North Atlantic temperate waters (19) are included for comparison.

classes of plastidic protists were operationally differentiated by flow cytometry using cell 90° light scatter, DNA content, and autofluorescence (Fig. S1).

Bacterioplankton cells were labeled using a pulse chase of two amino acids, [^{35}S]methionine and [^{3}H]leucine (*Materials and Methods*), to examine digestion of prey biomass by protist predators (*SI Text*). In the majority of experiments, in all regions studied, tracer content of protist cells increased with time during the chase phase in contrast to stable or slightly decreased tracer content of bacterioplankton cells (Figs. S2–S4). The increase demonstrates bacterivory by the three types of protist cells. More robust ^{35}S-based assessments (*SI Text*) were used to compare protist bacterivory in different oceanic regions (Fig. 2). Because only two stations were examined on each cruise in the Southern temperate (ST) region in austral spring, the 2008, 2009, and 2010 measurements were combined to get a more representative average estimate of protist bacterivory. The rates of bacterivory compared favorably with independent estimates (*SI Text*) derived from cell-uptake rates of phosphate in surface waters of the Northern subtropical gyre (NG). Moreover, the influence of light and dark incubation on bacterivory was studied on the cruise in 2010. No statistically significant light-induced differences (*t* test, $P > 0.1$) in protist bacterivory were determined (Fig. S2, SG 2010).

The rates of cell bacterivory (i.e., the number of bacterioplankton cells consumed per protist cell·h^{-1}) by the Aplast protists were comparable in all regions apart from the Northern temperate (NT) region in summer (Fig. 2). The difference between the ST and the NT regions was probably seasonal. Bacterivory by the Plast-L cells was the lowest in the Southern subtropical gyre (SG) in 2008 and 2010 but was comparable to bacterivory by Aplast cells in the ST region. Bacterivory by the Plast-S cells was lowest in temperate waters and in the SG in 2010. It was similar to bacterivory by the Plast-L cells in the NG in 2009 and in the SG in 2008, but lower in the SG in 2009 and 2010.

Rates of bacterivory in the SG varied interannually. Cell bacterivory by all three types of protists was significantly higher in 2009 compared with 2008 and 2010, whereas the differences between 2008 and 2010 were insignificant (Fig. 2). On the other hand, the concentration/biomass of the Plast-S population and the concentration of bacterioplankton were comparable between the 3 y (Fig. 3*A* and Fig. S5), whereas the concentration/biomass of Aplast and the Plast-L protists was higher in 2010. For comparison, *Synechococcus* and *Prochlorococcus* concentrations were 70% and 50% higher in 2010 compared with 2008, respectively (Fig. 1 *B–D* and Fig. S6). Bacterioplankton, *Synechococcus*, and *Prochlorococcus* concentrations in the surface mixed layer of the two gyres were similar in 2009, whereas Plast-L and Aplast biomass was lower in the SG than in the NG, and the opposite was true for the Plast-S protists (Fig. 1*C* and Figs. S5 and S6). The biomass of Plast-L protists was highest in all regions, followed by the biomass of Aplast and Plast-S protists (Fig. 3 *A* and *B*). The combined biomass of the two plastidic protist groups made up between 65% and 90% of the combined biomass of the smallest protists (Fig. 3*B*).

In contrast to cell bacterivory, population bacterivory (i.e., the total number of bacterioplankton consumed ml^{-1}·h^{-1} by each

ECOLOGY

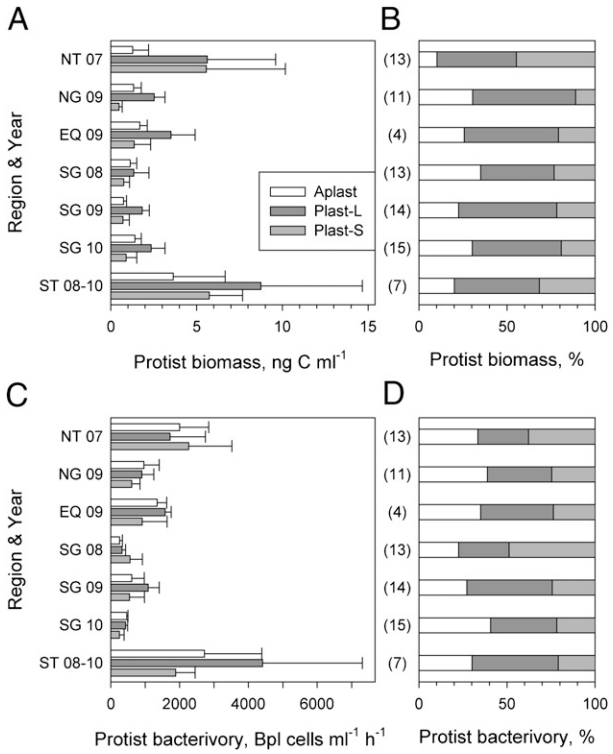

Fig. 3. A comparison of mean absolute (*A*) and relative (*B*) population biomass and mean absolute (*C*) and relative (*D*) population bacterivory of aplastidic, large plastidic, and small plastidic protists in the five regions (see Fig. 1 for details). The numbers next to the region abbreviations indicate the year of sampling. The numbers in parentheses indicate the number of experiments done in each region. The rates were calculated using [^{35}S]methionine pulse–chase tracing. Error bars show single SDs to indicate the variance of biomass and rates within regions.

protist population) in the NG and NT regions was not significantly different between the three protist populations (Fig. 3*C*). Population bacterivory was significantly higher in more productive temperate regions followed by the equatorial region (Fig. 3*C*), due to higher protist concentrations (Fig. 3*A* and Fig. S5). In the equatorial waters (EQ), and particularly in the SG in 2009, bacterivory by the Plast-L population was the highest compared with other populations, comprising 50% of total protist bacterivory (Fig. 3*D*). A comparison between the sum of plastidic populations and the aplastidic population showed a significant difference in population bacterivory by plastidic and aplastidic protists (*t* test, $P = 0.01$). Cumulative bacterivory by plastidic protists accounted for 60–77% of total protist bacterivory across the Atlantic Ocean. Furthermore, interannual variability had a minor effect on the domination of bacterivory by plastidic protists.

Discussion

The uniformly higher population rates of bacterivory by plastidic protists compared with aplastidic protists in the surface mixed layer of the Northern and Southern gyres and the equatorial region show the large contribution of phytoplankton to harvesting bacterioplankton in the low-latitude Atlantic Ocean. There are several important implications of this finding.

First, it challenges the long-standing assumption of the total dependence of phytoplankton on dissolved inorganic nutrients in oligotrophic oceanic waters. Independent culture studies have shown that some marine and freshwater algae can acquire scarce nutrients, such as phosphorus and iron, using bacterivory (22, 23). There are also field reports from nongyre regions that rates of bacterivory by plastidic protists between 3 and 5 μm and larger than 5 μm negatively correlate with the concentration of soluble reactive phosphorus or iron (16, 17). In this study, rates of bacterivory by Plast-S cells were lower in surface waters of the South Atlantic subtropical gyre compared with the North Atlantic subtropical gyre, which is depleted in phosphate (13). This suggests that the mixotrophy of Plast-S cells may be linked to phosphate depletion. However, differences linked to the seasonality of studies in the gyres (boreal autumn, austral spring) as well as interannual variability may also play a role here. In contrast, rates of bacterivory by Plast-L protists were comparable along the whole transect in 2009. Rates of bacterivory by Plast-L cells similar to those found in 2009 have also been measured in the temperate North Atlantic Ocean (19), further supporting the lack of correlation between macronutrient availability and bacterivory in Plast-L cells. The main temporal variability in Plast-L bacterivory was interannual in the SG. Both biomass and rates of bacterivory by Plast-L and Aplast populations are broadly comparable between the phosphate-depleted Northern and relatively phosphate-replete Southern Atlantic oligotrophic gyres (Fig. 3). This corroborates earlier observations of similar microbial abundance and bacterioplankton activities in the two gyres (24) (Fig. 1 and Fig. S5).

The second major implication of this work is related to the sustainability of oligotrophic ecosystems, because of the metabolic "inefficiency" of mixotrophs. Theoretically, mixotrophs require energy investment in both photosynthetic and phagotrophic cellular apparatus, and laboratory experiments suggest that they may be most ecologically successful when nutrient resources are limited (25) but light energy is plentiful, making surface waters of oligotrophic oceanic gyres their ideal habitat. High basic metabolic requirements and hence a decreased efficiency of nutrient retention by mixotrophic protist generalists compared with phototrophic or phagotrophic specialists (25, 26) should enhance rates of nutrient regeneration in the surface mixed layer of oligotrophic gyres. It has been claimed (26, 27) that by being mixotrophs, algae could also escape nutrient competition with bacterioplankton by reducing bacterioplankton concentrations to levels that would reduce or even arrest growth of specialist phagotrophs, such as aplastidic protists.

The third implication of our work is related to the cell metabolism of mixotrophs. Because CO_2 fixation as well as predation and respiration are concomitantly taking place in the same cells, mixotrophy could help to explain the tightness of biogenic carbon budgets at the community level (28). Tight intercellular coupling of production and respiration could contribute to the stability of oligotrophic ecosystems in the absence of seasonal or episodic perturbations (29) such as seasonally accumulated bioavailable organic matter (30), or allochthonous matter transported by advection (31) or deposited from the atmosphere (32, 33), which enhance growth of opportunistic species and ultimately change the composition of microbial communities.

The fourth implication concerns the ecological significance of the smallest plastidic protists in oligotrophic ecosystems. Apart from being key CO_2 fixers (5, 14), plastidic protists control bacterioplankton abundance, acting as producers of organic matter and predators at the same time. Such dual control and interdependence of bacterioplankton and protists could help to explain the constancy of low bacterioplankton concentrations in the oligotrophic ocean compared with more productive regions (34, 35). The scarcity of bacterioplankton prey in oligotrophic gyres in turn probably reduces both propagation of phage infections and growth of specialized predators such as aplastidic protists (Fig. S5).

In summary, this work shows the significance and ubiquity of mixotrophy in the survival of the smallest pelagic protists in sunlit oligotrophic surface waters. This deceptively inefficient lifestyle should reduce nutrient export and maintain faster nutrient turnover in the surface mixed layer, both of which are

essential for sustainable functioning of oligotrophic ecosystems. Consequently, future food web models should consider including mixotrophs as a basic ecosystem element.

Materials and Methods

Sampling. This study, comprising 68 experiments, was carried out in the Atlantic Ocean during one AMT cruise on board the UK Royal Research Ship (RRS) *James Clark Ross* in October–November 2008 and on two AMT cruises on board the UK RRS *James Cook* in October–November 2009 and 2010 (Fig. 1). Seawater samples were collected from a depth of 20 m before dawn with 20-L Niskin bottles mounted on a sampling rosette of a conductivity-temperature-depth profiler (Sea-Bird Electronics). In 2008 and 2009, experiments were set up within 20 min of sample collection in the dark at ambient temperature, controlled by a water bath to maintain temperature within 0.5 °C. In 2010, experiments were set up for dark and light measurements in a dark room using only a dim green light (LEE filter 090; transmission of 20–30% of light at 500–550 nm). Light incubation experiments were placed in a 6-L water tank illuminated by a warm white light-emitting diode (LED) array (Photon Systems Instruments). Parallel dark incubations were done in a similar water tank but were isolated from light. Both tanks were plumbed into a refrigerated bath (Grant Instruments) to maintain temperature within 0.5 °C of in situ temperature at the depth of sample collection. The LED array was adjusted to keep light intensity at 300 μmol photons $m^{-2}{\cdot}s^{-1}$ inside the incubation bottles.

Cell Counting. Bacterioplankton and protist cell concentrations were determined by flow cytometry (Fig. S1) using FACSort and FACSCalibur instruments (Becton Dickinson). *Synechococcus* and *Prochlorococcus* cyanobacteria were counted in unfixed samples (Fig. 1 *B–D* and Fig. S6). Concentrations of *Prochlorococcus* in the surface mixed layer were likely underestimated, owing to low chlorophyll content of cells that led to red autofluorescence of cells lying closer to the detection limit of the flow cytometers. The other samples were fixed with paraformaldehyde (PFA) 1% (wt/vol) final concentration and stained with SYBR Green I DNA dye (13, 36). A mixture of multifluorescent beads, of diameter 0.5 μm and 1.0 μm (fluoresbrite microparticles; Polysciences), was used as an internal standard for fluorescence and flow rates (37). To compare protist population biomass (Fig. 3 *A* and *B*), protist concentrations were multiplied by the corresponding cell biomass values.

To estimate their cell sizes, the three groups of protists were flow-sorted (Fig. S1), sorted cells being deposited on polycarbonate membrane filters with 0.2-μm pore diameter. Filters were mounted onto glass slides and stained excessively with DAPI (final concentration 1 $\mu g{\cdot}ml^{-1}$) to reveal cell cytoplasm. Aplast cells were sorted and sized from four experimental samples on the 2009 cruise and from five experimental samples on the 2010 cruise, which represented all regions studied. Plast-L and Plast-S cells were sorted from five and four experimental samples on the 2010 cruise, respectively. At least 200 cells were measured at 1,000× magnification of an epifluorescence microscope (Axioscope 2; Zeiss) to estimate mean cell diameters. Mean cell diameters of each of the three protist groups were statistically similar in analyzed samples (Table S1). The overall mean size of Plast-S cells of 2.0 ± 0.1 μm was significantly lower (*t* test, $P = 0.0002$) than the overall mean for Plast-L cells of 3.1 ± 0.3 μm, whereas the overall mean size of Aplast cells of 2.9 ± 0.3 μm was statistically similar to the size of Plast-L cells. To estimate the biomass of the three protist groups, their cell biovolume was computed assuming that the cells were spheres with a diameter equal to the mean cell size. Cell biovolume was converted into cell biomass using a specific carbon content of 200 fg $C{\cdot}\mu m^{-3}$, taken as a mean value from Christian and Karl (38).

Determining Rates of Protist Bacterivory Using Pulse–Chase Dual Labeling of Natural Communities. Before an experiment, glass bottles (250 mL, Schott; Fisher Scientific) were soaked in 10% hydrochloric acid and rinsed twice with 50 mL of sampled seawater (taken from the same Niskin bottle as that for the subsequent experiment). Seawater (250 mL) from the sample was subsequently added to each washed glass bottle and spiked with L-[^{35}S]methionine (specific activity >37 TBq/mmol; Hartmann Analytic), final concentration 0.25 nM or 0.4 nM, and L-[4,5-^{3}H]leucine (specific activity 1.48–2.22 TBq/mmol; Hartmann Analytic), final concentration 0.5 nM. An increase in the amount of label (and thus the sensitivity of the experiment) was necessary to compensate for the low abundance of protists in the oligotrophic gyres. After a 1.5-h incubation, nonradioactive methionine and leucine were added to final concentrations of 0.25 μM, or 0.4 μM and 0.5 μM, respectively, to chase the radioactive amino acids (19, 20). Samples were incubated for 1.5 h to stabilize pulses in bacterioplankton cells before taking subsamples [120 mL; fixed with 1% (wt/vol) PFA at 3 h and 9 h] for the measurement of protist tracer uptake rates. In parallel, the pulse chase was monitored over 9 h by taking 1.6-mL subsamples every 15 min for 3 h followed by sampling intervals of 1 h until the end of the 9-h experiment. These samples were fixed with 1% (wt/vol) PFA and, after 1 h of fixation, particulate material was collected onto 0.2-μm polycarbonate filters (Nuclepore; Whatman) to measure the total sample radioactivity (Figs. S7 and S8).

In addition to the two-point experiments (3 h vs. 9 h), time-course experiments were carried out at several stations on two cruises (2008 and 2009) with samples fixed at four time points for subsequent population sorting to resolve protist feeding dynamics (Figs. S3 and S9).

To check for potential osmotrophic uptake of tracers by protists during the chase phase, additional so-called chase–pulse experiments (in parallel to "pulse–chase" experiments) were carried out at three stations on the 2009 cruise. In the "chase–pulse" experiments, samples were initially spiked with unlabeled leucine and methionine molecules at concentrations of radiotracers used in the parallel pulse–chase experiment. After a 1.5-h incubation, unlabeled amino acids were added at concentrations to match the values used in the chase (see above), and in addition radiotracers were added at concentrations identical to the ones used in the pulse phase. Subsamples were fixed for flow sorting after 3 h and 9 h. The measured radioactivity in chase–pulse–labeled and –sorted cells was comparable to the background (Fig. S4), confirming the insignificant osmotrophic uptake of tracer molecules by sorted protists and bacterioplankton during the chase phase.

Flow Cytometric Cell Sorting. PFA-fixed radioactively labeled samples were stored at 4 °C and sorted within 10 h. For each time point, four different populations (total bacterioplankton, Plast-S, Plast-L, and Aplast protists) were sorted (Fig. S1). For each population, four to eight replicates of different cell numbers were sorted (19).

Sorted bacterioplankton cells were collected onto 0.2-μm polycarbonate filters. Sorted protist cells were collected onto 0.8-μm polycarbonate filters to reduce the retention of potentially by-sorted Bpl cells. Filters were washed with deionized water to remove contaminating tracer and placed into scintillation vials to which 5 mL of scintillation mixture (GoldStar) was added. Subsequently, the vials were radioassayed for 0.5–2 h (depending on sample radioactivity) using ultra–low-level liquid scintillation counters (1220 Quantalus; Wallac).

Data Analyses. Using quench curves, the ^{3}H label was deconvoluted from the ^{35}S label, and the amount of each label was computed as $Bq{\cdot}cell^{-1}$ by dividing the cumulative ^{3}H or ^{35}S radioactivity by the corresponding number of sorted cells. Cell radioactivities at 3 h and 9 h were compared including dark and light incubations (Fig. S2).

Cell bacterivory was calculated according to the following formula:

$$\text{Bacterivory} = \left(\text{Prt}_{\text{avg}}\text{T2} \times \text{Bpl}_{\text{avg}}\text{T2}^{-1} - \text{Prt}_{\text{avg}}\text{T1} \times \text{Bpl}_{\text{avg}}\text{T1}^{-1}\right) \times (\text{T2} - \text{T1})^{-1},$$

where Prt_{avg}T2 is the average activity of four to eight replicates of one of the protist groups at the second time point and Prt_{avg}T1 is the same at the first time point; T1 and T2 are the first and second time points of the experiment (e.g., 3 h and 9 h, respectively); Bpl_{avg}T1 and Bpl_{avg}T2 are the average activity of four to eight replicates of the bacterioplankton cells at T1 and T2, respectively. Because of the pulse–chase experimental design, the activity of the Bpl was in most cases the same at T1 and T2 (Figs. S2–S4) and a cumulative mean could be used.

To verify that the increase in label between the first and second time points was statistically significant, *t* tests ($P < 0.05$) were carried out using SigmaPlot version 11.0 (Systat Software) and Quattro-Pro X4 (Corel) software. Errors were calculated according to SE propagation procedures. The majority of experiments (80%) showed a significant difference in protist radioactivity between the two time points (Figs. S2 and S4) and hence demonstrated bacterivorous activity of the Plast-S, Plast-L, and Aplast cells. We attribute nonsignificant bacterivory in some experiments to the detection limit of our method owing to the low radioactivities measured. All estimates of rates of cell bacterivory were included in calculations of average regional rates (Fig. 2). The mean rates were all significantly higher than zero (*t* tests, $P < 0.05$). To calculate regional bacterivory of the protist populations (Fig. 3*C*), bacterivory per cell was multiplied by the corresponding mean concentration of protist $cells{\cdot}ml^{-1}$. *t* tests were used to compare mean values; SDs, derived from pooled variance, are used to show variability within regions (Figs. 2 and 3).

ACKNOWLEDGMENTS. We thank the captains, officers, and crew aboard the RRS *James Clark Ross* and the RRS *James Cook* for their help during the three cruises. We thank Michael Sleigh for his encouragement and critical comments on an earlier draft of the paper. This study was supported by the UK Natural Environment Research Council through Research Grants NE/E016138/1 and NE/G005125/1, the Oceans 2025 Core Programme of the National Oceanography Centre and Plymouth Marine Laboratory, and the European Commission Seventh Framework Programme through the GreenSeas Collaborative Project (FP7-ENV-2010 Contract 265294). This is Atlantic Meridional Transect Publication no. 214.

1. Polovina JJ, Howell EA, Abecassis M (2008) Ocean's least productive waters are expanding. *Geophys Res Lett* 35:L03618.
2. Chisholm SW, et al. (1988) A novel free-living prochlorophyte abundant in the oceanic euphotic zone. *Nature* 334:340–343.
3. Morris RM, et al. (2002) SAR11 clade dominates ocean surface bacterioplankton communities. *Nature* 420:806–810.
4. Cuvelier ML, et al. (2010) Targeted metagenomics and ecology of globally important uncultured eukaryotic phytoplankton. *Proc Natl Acad Sci USA* 107:14679–14684.
5. Jardillier L, Zubkov MV, Pearman J, Scanlan DJ (2010) Significant CO_2 fixation by small prymnesiophytes in the subtropical and tropical northeast Atlantic Ocean. *ISME J* 4: 1180–1192.
6. Lepère C, Vaulot D, Scanlan DJ (2009) Photosynthetic picoeukaryote community structure in the South East Pacific Ocean encompassing the most oligotrophic waters on Earth. *Environ Microbiol* 11:3105–3117.
7. Liu H, et al. (2009) Extreme diversity in noncalcifying haptophytes explains a major pigment paradox in open oceans. *Proc Natl Acad Sci USA* 106:12803–12808.
8. Shi XL, Lepère C, Scanlan DJ, Vaulot D (2011) Plastid 16S rRNA gene diversity among eukaryotic picophytoplankton sorted by flow cytometry from the South Pacific Ocean. *PLoS One* 6:e18979.
9. Zubkov MV, Burkill PH, Topping JN (2007) Flow cytometric enumeration of DNA-stained oceanic planktonic protists. *J Plankton Res* 29(1):79–86.
10. Azam F, et al. (1983) The ecological role of water-column microbes in the sea. *Mar Ecol Prog Ser* 10:257–263.
11. Chisholm SW (1992) Phytoplankton size. *Primary Productivity and Biogeochemical Cycles in the Sea*, eds Falkowski PG, Woodhead AD (Plenum, New York), pp 213–237.
12. Hartmann M, et al. (2011) Comparison of phosphate uptake rates by the smallest plastidic and aplastidic protists in the North Atlantic subtropical gyre. *FEMS Microbiol Ecol* 78:327–335.
13. Zubkov MV, et al. (2007) Microbial control of phosphate in the nutrient-depleted North Atlantic subtropical gyre. *Environ Microbiol* 9:2079–2089.
14. Li WKW (1994) Primary production of prochlorophytes, cyanobacteria, and eukaryotic ultraphytoplankton: Measurements from flow cytometric sorting. *Limnol Oceanogr* 39(1):169–175.
15. Christaki U, Van Wambeke F, Dolan JR (1999) Nanoflagellates (mixotrophs, heterotrophs and autotrophs) in the oligotrophic eastern Mediterranean: Standing stocks, bacterivory and relationships with bacterial production. *Mar Ecol Prog Ser* 181: 297–307.
16. Stukel MR, Landry MR, Selph KE (2011) Nanoplankton mixotrophy in the eastern equatorial Pacific. *Deep Sea Res Part II Top Stud Oceanogr* 58:378–386.
17. Unrein F, Massana R, Alonso-Saez L, Gasol JM (2007) Significant year-round effect of small mixotrophic flagellates on bacterioplankton in an oligotrophic coastal system. *Limnol Oceanogr* 52:456–469.
18. Frias-Lopez J, Thompson A, Waldbauer J, Chisholm SW (2009) Use of stable isotope-labelled cells to identify active grazers of picocyanobacteria in ocean surface waters. *Environ Microbiol* 11:512–525.
19. Zubkov MV, Tarran GA (2008) High bacterivory by the smallest phytoplankton in the North Atlantic Ocean. *Nature* 455:224–226.
20. Zubkov MV, Sleigh MA (1995) Ingestion and assimilation by marine protists fed on bacteria labeled with radioactive thymidine and leucine estimated without separating predator and prey. *Microb Ecol* 30:157–170.
21. Zubkov MV, Sleigh MA (2005) Assimilation efficiency of *Vibrio* bacterial protein biomass by the flagellate *Pteridomonas*: Assessment using flow cytometric sorting. *FEMS Microbiol Ecol* 54:281–286.
22. Kamjunke N, Henrichs T, Gaedke U (2007) Phosphorus gain by bacterivory promotes the mixotrophic flagellate *Dinobryon* spp. during re-oligotrophication. *J Plankton Res* 29(1):39–46.
23. Maranger R, Bird DF, Price NM (1998) Iron acquisition by photosynthetic marine phytoplankton from ingested bacteria. *Nature* 396:248–251.
24. Zubkov MV, Sleigh MA, Burkill PH, Leakey RJG (2000) Bacterial growth and grazing loss in contrasting areas of North and South Atlantic. *J Plankton Res* 22:685–711.
25. Rothhaupt KO (1996) Laboratory experiments with a mixotrophic chrysophyte and obligately phagotrophic and phototrophic competitors. *Ecology* 77:716–724.
26. Tittel J, et al. (2003) Mixotrophs combine resource use to outcompete specialists: Implications for aquatic food webs. *Proc Natl Acad Sci USA* 100:12776–12781.
27. Thingstad TF, Havskum H, Garde K, Riemann B (1996) On the strategy of "eating your competitor": A mathematical analysis of algal mixotrophy. *Ecology* 77:2108–2118.
28. Williams PJL (1998) The balance of plankton respiration and photosynthesis in the open oceans. *Nature* 394:55–57.
29. Karl DM, Laws EA, Morris P, Williams PJL, Emerson S (2003) Global carbon cycle: Metabolic balance of the open sea. *Nature* 426(6962):32.
30. Thingstad TF, et al. (2005) Nature of phosphorus limitation in the ultraoligotrophic eastern Mediterranean. *Science* 309:1068–1071.
31. Roussenov V, Williams RG, Mahaffey C, Wolff GA (2006) Does the transport of dissolved organic nutrients affect export production in the Atlantic Ocean? *Global Biogeochem Cycles* 20:GB3002.
32. Calil PHR, Doney SC, Yumimoto K, Eguchi K, Takemura T (2011) Episodic upwelling and dust deposition as bloom triggers in low-nutrient, low-chlorophyll regions. *J Geophys Res* 116:C06030.
33. Dachs J, et al. (2005) High atmosphere-ocean exchange of organic carbon in the NE subtropical Atlantic. *Geophys Res Lett* 32:L21807.
34. Li WKW, Head EJH, Harrison WG (2004) Macroecological limits of heterotrophic bacterial abundance in the ocean. *Deep Sea Res Part I Oceanogr Res Pap* 51: 1529–1540.
35. Zubkov MV, Tarran GA, Mary I, Fuchs BM (2008) Differential microbial uptake of dissolved amino acids and amino sugars in surface waters of the Atlantic Ocean. *J Plankton Res* 30:211–220.
36. Marie D, Partensky F, Jacquet S, Vaulot D (1997) Enumeration and cell cycle analysis of natural populations of marine picoplankton by flow cytometry using the nucleic acid stain SYBR Green I. *Appl Environ Microbiol* 63(1):186–193.
37. Zubkov MV, Burkill PH (2006) Syringe pumped high speed flow cytometry of oceanic phytoplankton. *Cytometry A* 69:1010–1019.
38. Christian JR, Karl DM (1994) Microbial community structure at the U.S.-Joint Global Ocean Flux Study Station ALOHA: Inverse methods for estimating biochemical indicator ratios. *J Geophys Res* 99:14269–14276.